

## A NEW BOUNDARY CONDITION FOR THE EVALUATION OF HYDROGEN TRANSPORT IN METALS USING AN ELECTROCHEMICAL TECHNIQUE

João Flávio Vieira de Vasconcellos<sup>1</sup>

Sílvia Inez Carvalho<sup>2</sup>

Ivan Napoleão Bastos<sup>3</sup>

Department of Mechanical Engineering and Energy

Instituto Politécnico, IPRJ, Universidade do Estado do Rio de Janeiro, UERJ

P.O. 97282, 28601-970, Nova Friburgo, RJ, Brazil

<sup>1</sup>jflavio@iprj.uerj.br, <sup>2</sup>silviainezcarvalho@yahoo.com.br, <sup>3</sup>inbastos@iprj.uerj.br

Dilson Silva dos Santos<sup>4</sup>

Programa de Pós-Graduação em Engenharia Metalúrgica e de Materiais

Instituto Alberto Luiz Coimbra de Pós Graduação e Pesquisa de Engenharia, Universidade Federal do Rio de Janeiro

Rua Brigadeiro Trompowsky s/n Bloco F sala 210, Centro de Tecnologia - Ilha do Fundão

21945-970 – Rio de Janeiro, RJ - Brasil – P.O 68505

<sup>4</sup>dilson@metalmat

**Abstract.** *Some metals and alloys solubilize hydrogen during service, and this absorption can reduce their mechanical properties. To evaluate the susceptibility of metals to hydrogen degradation the procedures prescribed in ASTM G148-97 standard are used. However, some interfacial and volumetric phenomena occurred in metal and the conditions considered in analytical solutions of this standard are no longer valid. In this sense, new boundary conditions are proposed to fit experimental results with the simulated. The solution of the Fick equation with these new conditions needs a numerical solution, and a computational modeling used finite elements to solve the equation with this new situation. The simulated results are compared with experimental one and they agree very well.*

**Keywords:** *hydrogen diffusion, boundary conditions, numerical solution*

### 1. Introduction

It is well known that the presence of hydrogen causes a severe degradation of mechanical properties of some materials. For example, reactors that are exposed to a high hydrogen pressure and to elevated temperatures often suffer from the material degradation process called hydrogen attack. Carbon in the steel reacts with hydrogen that has diffused in from the gas atmosphere inside the reactor, to form methane. These molecules are captured in cavities that have nucleated at the grain boundaries. Due to the presence of methane and hydrogen molecules, the cavities are internally pressurized. Consequently, the cavities grow and coalesce which finally results in intergranular fracture (Schlögl and Van der Giessen, 2002). Hydrogen in alloy also can cause catastrophic failure via hydrogen embrittlement or blistering.

Devanathan and Stachurski (1962) have first developed an electrochemical technique that has been successfully used to measure the effective hydrogen diffusivity and permeability in many ferritic and martensitic iron based alloys. Nowadays, the transport of hydrogen in metals is evaluated by electrochemical technique (ASTM G148-97, 1997), which was developed based mostly on Devanathan and Stachurski (1962) work. This practice can be applied in principle to all metals and alloys which have a high solubility for hydrogen, and for which the hydrogen permeation is measurable. This method can be used to rank the relative aggressivity of different environments in terms of the hydrogen uptake of the exposed metal.

Both works, Devanathan and Stachurski (1962) and ASTM G148-97 (1997), are based on the analytical solution of the Fick equation,

$$\frac{\partial C}{\partial t} = D \frac{\partial^2 C}{\partial x^2} \quad (1)$$

where  $C$  is the concentration of hydrogen,  $D$  is the diffusion coefficient,  $L$  is the sample thickness, and  $t$  and  $x$  are the temporal and spatial variables respectively. Equation (1) is supplemented by the following boundary and initial conditions

$$\begin{aligned} C(x=0, t) &= C_0 & (x=0 \text{ is the surface at the cathodic side}) \\ C(x=L, t) &= 0 & (x=L \text{ is the surface at the anodic side}) \\ C(x, t=0) &= 0 \end{aligned} \quad (2)$$

and  $C_0$  is the concentration of hydrogen in the cathodic side. The analytical solution of the hydrogen permeation current density,  $j(t)$ , is defined as following

$$j(t) = -DF \left. \frac{\partial C}{\partial x} \right|_{x=L} = -\frac{DF C_0}{L} \left( 1 + 2 \sum_{n=1}^{\infty} (-1)^n e^{-\left(\frac{D}{L^2} n^2 \pi^2\right) t} \right) \quad (3)$$

where  $F$  is the Faraday constant. It can be seen in Fig. 1 a typical plot of Eq. (3), and the current density obtained experimentally by Velasco (2003) is shown in Fig. 2. In this work, Velasco employed solutions of sulphuric and acetic acids. It is clear that the behavior of the current density in both curves is quite different. Fig. 1 shows that after a delay the anodic current density increases from zero up to its final steady-state value, and this behavior is normally found in NaOH electrolyte. This delay depends on the insertion reaction kinetics, diffusion coefficient and sample thickness. The experimental data, Fig. 2, does not show the same behavior, that is, the steady-state value was not achieved in this experiment and, therefore, the theoretical curve does not fit the experimental data as well as it should to estimate the diffusion process correctly.

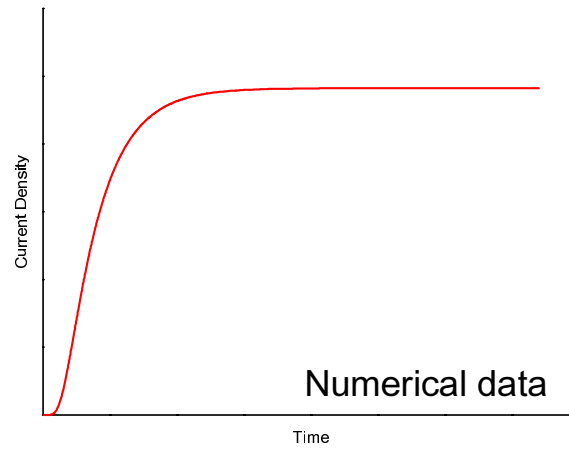


Figure 1 – Typical plot of permeation current density using Eq. (3).

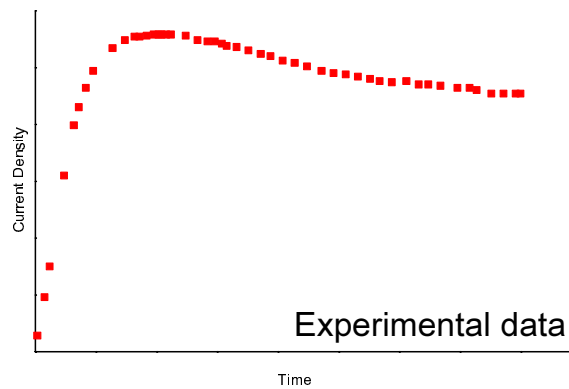


Figure 2 – Experimental data obtained by Velasco (2003).

In this paper it is shown that usual boundary conditions may not express satisfactorily the physical phenomenon in the anodic side of the sample. Afterward, a new boundary condition is proposed to Eq. (1). In the results section, it will be shown that the new boundary condition allows a better agreement between numerical and experimental data. There will be also a discussion about what is taking place in the anodic sample and why Eq. (3) is not a good boundary condition for this problem.

## 2. The New Boundary Condition

The steady-state solution of Eq. (1) for the boundary conditions described by Eqs. (2) and (3) is

$$C(x) = C_0 \left( \frac{L-x}{L} \right) \quad (4)$$

and as a result,

$$\left. \frac{\partial C}{\partial x} \right|_{x=L} = -\frac{C_0}{L} \quad (5)$$

Equation (5) clearly affirms that the term  $\left. \frac{\partial C}{\partial x} \right|_{x=L}$  becomes constant when time tends to infinity, thus, analyzing Eq. (3), the value of  $j(t)$  also turns out to be constant. This explains the constant value of the hydrogen permeation current density in Fig. 1. At this point, it is possible to understand why the results obtained with Eqs. (1), (2) and (3) will never fit the experimental data shown in Fig. 2.

The solution proposed by Carvalho (2005) and Vasconcellos *et alii* (2005) is to use a new boundary condition, which should be used in place of Eq. (3),

$$C(x=L, t) = \langle C_f (1 - e^{-\nu(t-t_0)}) \rangle \quad (6)$$

where the function  $\langle x \rangle$  is defined as

$$\langle x \rangle = 0 \text{ if } x < 0 \text{ and } \langle x \rangle = x \text{ if } x > 0 \quad (7)$$

and  $C_f$ ,  $\nu$  and  $t_0$  are constants and  $\nu$  is used to control how fast hydrogen concentration changes. The plot of Eq. (6) is shown in Fig. 3.

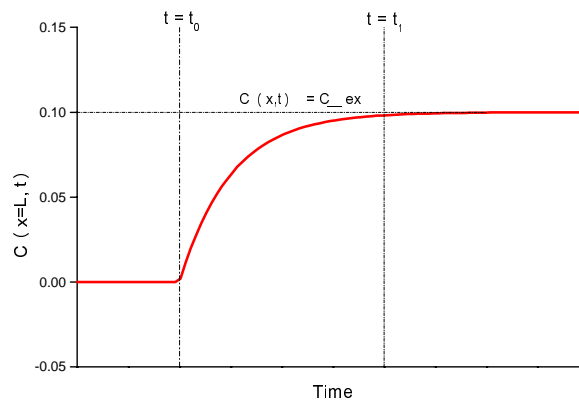


Figure 3 – Plot of Eq. (6)

To the authors' knowledge, no other research has been conducted on this topic using an equation like Eq. (6). From a mathematical point of view, Eq. (6) has some characteristics that Eq. (3) does not, *i.e.*,

1. Eq. (6) is not constant with respect with time during the time interval from  $t_0$  to  $t_1$  (see Fig. 3). As a consequence of this,  $\left. \frac{\partial C}{\partial x} \right|_{x=L}$  and  $j(t)$  are not constants during the interval from 0 to  $t_1$ .

2. The function  $\langle x \rangle$  is necessary to avoid non-physical negative current density. Without this function, the value of  $C(x, t)$  is bigger at the boundary than at the interior, thus  $\left. \frac{\partial C}{\partial x} \right|_{x=L}$  is positive and  $j(t)$  negative.

Eq. (6) was not chosen arbitrarily instead of Eq. (3). This equation is based on the idea that the hydrogen concentration in the anodic side of the sample has neither null nor constant value. The physical reasoning of this is that due to the anodic potential forced by a potentiostat, an oxide film can form; and avoid the hydrogen concentration to be null. Besides, this concentration increases as the experiment time passes affected by growth of anodic film.

### 3. Solution Methodology

Analytical methods had been used to solve one-dimensional diffusion equations like Eq. (1). In this work it was used a numerical procedure to solve the dimensionless form of Eq. (1) mainly because the model presented herein will be improved to solve more complex situation. In this sense, the dimensionless diffusion coefficient is dependent of its position. The dimensionless form of Eq. (1) is

$$\frac{\partial \phi}{\partial \tau} = \frac{\partial}{\partial \xi} \left[ \Gamma \frac{\partial \phi}{\partial \xi} \right] \quad (8)$$

and the boundary and initial conditions are

$$\phi(\xi = 0, \tau) = 1 \text{ for } \tau > 0 \quad (9)$$

$$\phi(\xi = 1, \tau) = \left\langle \phi_f \left( 1 - e^{-\alpha(\tau - \tau_0)} \right) \right\rangle \text{ for } \tau > 0 \quad (10)$$

$$\phi(\xi, \tau = 0) = 0 \text{ for } 0 \leq \xi \leq 1 \quad (11)$$

where

$$\begin{aligned} \phi &= \frac{C}{C_0}, \quad \phi_f = \frac{C_f}{C_0} \\ \tau &= \frac{D_{ref}}{L^2} t, \quad \tau_0 = \frac{D_{ref}}{L^2} t_0 \\ \Gamma &= \frac{D}{D_{ref}}, \quad \xi = \frac{x}{L}, \text{ and } \alpha = v \frac{L^2}{D_{ref}} \end{aligned} \quad (12)$$

The hydrogen permeation current density,  $j(t)$ , is now defined as following

$$j(t) = -FC_0 \frac{\Gamma D_{ref}}{L} \left. \frac{\partial \phi}{\partial \xi} \right|_{\xi=1} \quad (13)$$

In the present work, Eq. (8) was solved numerically using the Finite Volume Method (Patankar, 1980; Ferziger and Peric, 1996). In this methodology, the first step is to divide the solution domain in small non-overlapping control volumes, whose faces are aligned with the coordinate lines. Details about the grid used in this work are shown in Fig. 4. Next, the equations are integrated along each one of these control volumes yielding a set of algebraic equations. The concentration derivatives along the faces of the control volumes are approximated using piecewise linear profiles, and after rearrangements all algebraic equations are cast into the following formula

$$A_P \phi_P = A_e \phi_e + A_w \phi_w + S_P \quad (14)$$

where the subscript  $P$  refers to the control volume properly which neighbors are at **E**ast and **W**est;  $S_P$  is a source term. For all internal volumes, the coefficients of Eq. (14) are

$$A_e = \frac{\Gamma}{\delta\xi_e}, \quad A_w = \frac{\Gamma}{\delta\xi_w}, \quad S_p = \frac{\Delta\xi_p}{\Delta\tau} \phi_p^0 \text{ and } A_p = \frac{\Delta\xi_p}{\Delta\tau} + A_e + A_w \quad (15)$$

and for the first volume, coefficients of Eq. (14) are

$$A_e = \frac{\Gamma}{\delta\xi_e}, \quad A_w = 0, \quad S_p = \frac{\Delta\xi_p}{\Delta\tau} \phi_p^0 + \frac{\Gamma}{\delta\xi_w} \text{ and } A_p = \frac{\Delta\xi_p}{\Delta\tau} + A_e \quad (16)$$

and, for the last volume, the coefficients of Eq. (14) are

$$A_e = \frac{\Gamma}{\delta\xi_e}, \quad A_w = \frac{\Gamma}{\delta\xi_w}, \quad S_p = \frac{\Delta\xi_p}{\Delta\tau} \phi_p^0 + \frac{\Gamma}{\delta\xi_w} \left\langle \phi_f \left( 1 - e^{-\alpha(\tau - \tau_0)} \right) \right\rangle \text{ and } A_p = \frac{\Delta\xi_p}{\Delta\tau} + A_w \quad (17)$$

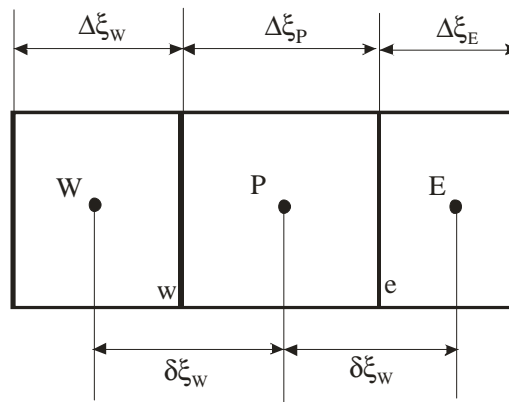


Figure 4 – Typical control volume used to integrate Eq. (8).

The linear system of equations formed by Eqs. (14)-(17) was solved using the Thomas algorithm – TDMA – (Patankar, 1980). The following is a brief description of the numerical procedures:

1. Set initial values of the dependent variable:  $\phi$
2. Calculate the coefficients and source terms for  $\phi$
3. Solve the corresponding linear system, Eq. (14), obtaining  $\phi_p$  for  $1 \leq P \leq N$ , where  $N$  is the number of volumes used to descriptive the domain.
4. If the steady-state is achieved, the computation ended. Otherwise, forward to the next time step and redo the Steps 2 and 3.

Figure 5 shows the excellent fit between analytical solution of standard case and the numerically simulated curve.

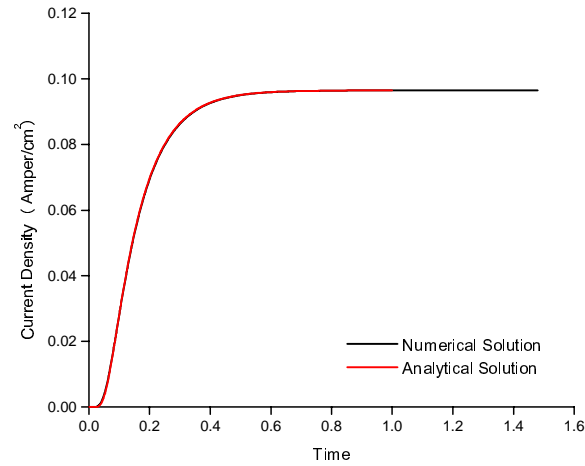


Figure 5 – Comparison between numerical model results and analytical solution.

#### 4. Results and Discussions

The validation of the present scheme was performed by comparing the results obtained here with those available in the literature. For  $\phi_f = 0$  Eq. (8) becomes equal to Eq. (3) and then it is possible to compare the numerical solution presented herein with an analytical solution of the differential equation, Eq. (1). It can be seen a good agreement between the results of both models numerical and analytical. Some other numerical experiments were conducted by Carvalho (2005) to understand the behavior of the numerical procedure presented in this work but they are not discussed here for lack of space.

In this work, it was used experimental data to simulate realistic conditions. The data of hydrogen permeation current density were obtained from Velasco (2003) and Bruzzoni *et alii* (1992).

Figure 6 shows experimental data obtained from Vellasco and co-worker (1992) that used ASTM A516 Gr.60 steel and a sample thickness of  $L = 1$  mm. In Table 1 are shown all parameter used to perform the simulation. These values were obtained using an inverse problem technique that is presented in Carvalho (2005).

Table 1 – Parameters used to fit the data from Velasco (2003).

Parameter	$\alpha$	$C_0$ (mol/cm <sup>3</sup> )	$C_f$ (mol/cm <sup>3</sup> )	$D$ (cm <sup>2</sup> /s)	$\tau_0$
Value	0.01	$8.963 \times 10^{-7}$	$8.697 \times 10^{-6}$	$3.487 \times 10^{-6}$	0.1

Figure 6 shows the results of this simulation and it is clear that there is a very good agreement with numerical and experimental data. This agreement also can be found in the Fig. 7 where it was used experimental data from Bruzzoni *et alii* (1992). The experiment performed by Bruzzoni *et alii* (1992) had also used ASTM A516 Gr.60 steel and a sample thickness of  $L = 0.48$  mm.

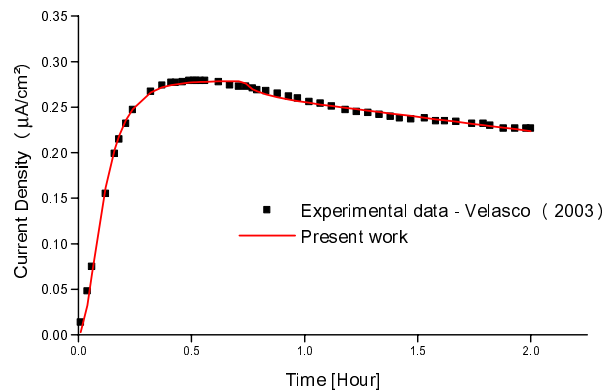


Figure 6 – Hydrogen permeation current density curves obtained with the procedure presented herein and experimental data from Velasco (2003).

Table 2– Parameters used to fit the data from Bruzzoni *et alii* (1992).

Parameter	$\alpha$	$C_0$ (mol/cm <sup>3</sup> )	$C_f$ (mol/cm <sup>3</sup> )	$D$ (cm <sup>2</sup> /s)	$\tau_0$
Value	0.01	$1.030 \times 10^{-6}$	$2.796 \times 10^{-6}$	$1.989 \times 10^{-7}$	$1.00 \times 10^{-5}$

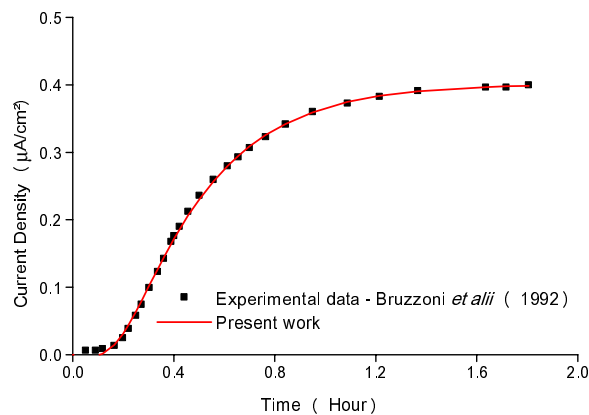


Figure 7 – Hydrogen permeation current density curves obtained with the procedure presented herein and experimental data from Bruzzoni *et alii* (1992).

It is important to note that when the film is thin, with approximately 1% of sample thickness, the effect of film diffusion coefficient is negligible, thus insufficient to model a permeation decay as observed here (Carvalho, 2005). Therefore, it is necessary to consider a non-null concentration of anodic side to fit the curve.

## 5. Conclusion

To model the hydrogen permeation curves with electrochemical technique when the steady-state are not achieved is proposed an evolution law of surface concentration that varies with permeation time. With this boundary condition it is necessary a numerical procedure to solve the Fick equation. Thus, a Finite Volume Method was implemented and performed. The results were compared with two experiment examples and fit very well. As a result it is possible to show that the type of curve studied here is necessary to take into account the non-null concentration of hydrogen on anodic side.

#### 4. Acknowledgements

Financial support was received from CAPES, FAPERJ and CNPq Brazilian agencies.

#### 5. References

- ASTM G148-97, 1997, “Standard Practice for Evaluation of Hydrogen Uptake, Permeation, and Transport in Metals by an Electrochemical Technique”, ASTM International.
- Bruzzoni, P. and Garavalia, R., 1992, “Anodic Iron Oxide Films and Their Effect on the Hydrogen Permeation Through Steel”, *Corrosion Science*, 33, 11, pp.1797-1807.
- Carvalho, S. I., 2005, “Simulação de Difusão de Hidrogênio em Metais”, Dissertação de Mestrado, Programa de Pós-Graduação em Modelagem Computacional, IPRJ/UERJ, Nova Friburgo, Rio de Janeiro. *{in portuguese}*
- Devanathan, M.A.V. and Stachurski, Z., 1962, “The Adsorption and Diffusion of Electrolytic Hydrogen in Palladium”. *The Electrochemistry*, Laboratory University of Pennsylvania, Philadelphia, pp. 90–102.
- Ferziger, J. H. and Peric, M., 1996, *Computational Methods for Fluid Dynamics*, Springer, Berlin.
- Patankar, S. V., 1980, *Numerical Heat Transfer and Fluid Flow*, Hemisphere Publishing Co., Washington D.C.
- Schlögl S. M. and Van der Giessen, E., 2002, “Computational Model for Carbon Diffusion and Methane Formation in a Ferritic Steel During Hydrogen Attack”, *Scripta Materialia*, Vol. 46, pp. 431–436.
- Vasconcellos, J. F. V., Carvalho, S. I., Bastos, I. N. and Santos, D. S., 2005, “Simulação de Difusão de Hidrogênio em Materiais Metálicos”, VIII Conferência sobre Tecnologia de Equipamentos – COTEQ 2005, Salvador, Bahia. *{in portuguese}*
- Velasco, J. A. C., 2003, “Alguns Aspectos sobre o Cálculo do Coeficiente de Difusão de Hidrogênio no Aço ao Carbono via Impedância Eletroquímica e Permeação”, Dissertation thesis, COPPE/UFRJ, Rio de Janeiro. *{in portuguese}*.

#### 6. Responsibility notice

The authors are the only responsible for the printed material included in this paper.